Metal contacts in carbon nanotube field-effect transistors: Beyond the Schottky barrier paradigm

J. J. Palacios,[1] P. Tarakeshwar,[2] and Dae M. Kim[2]
[1]*Departamento de Física Aplicada, Universidad de Alicante, Campus de San Vicente del Raspeig, E-03690 Alicante, Spain*
[2]*School of Computational Sciences, Korea Institute for Advanced Study, Cheongnyangni-2-dong, Dongdaemun-gu, 207-43 Seoul, Republic of Korea*

(Received 11 October 2007; revised manuscript received 8 November 2007; published 12 March 2008)

The observed performances of carbon nanotube field-effect transistors are examined using first-principles quantum transport calculations. We focus on the nature and role of the electrical contact of Au and Pd electrodes to open-ended semiconducting nanotubes, allowing the chemical contact at the surface to fully develop through large-scale relaxation of the contacting atomic configuration. As expected from their respective work functions, the Schottky barrier heights for Au and Pd turn out to be fairly similar for realistic contact models. We present, however, direct numerical evidence of Pd contacts exhibiting perfect transparency for hole injection as opposed to that of Au contacts. These findings support experimental data reported to date.

DOI: 10.1103/PhysRevB.77.113403 PACS number(s): 73.63.Fg, 73.40.Sx

The superb performances of carbon nanotube (CNT) field-effect transistors have been demonstrated over the past decade.[1–8] However, a number of factors determining the current-voltage (*I-V*) characteristics have to be clarified for extensive device applications. A key factor in this context is the Schottky barrier (SB) formed at the interface between the source and drain metallic electrodes and the CNT. Traditionally, Schottky contacts have been introduced to serve as passive ohmic contacts. However, Schottky contacts in CNT field-effect transistors play an active role in affecting the transistor action. For example, the drastic disparity of reported performances of CNT transistors has generally been attributed to the difficulty in controlling the position of the Fermi energy E_F with respect to the valence and conduction bands of the CNTs, when they are brought into contact to metal electrodes via different fabrication processes.[9,10] The different E_F locations should in turn give rise to different SB's and hence different *I-V* behaviors.

In the simplest Mott and/or Schottky picture for metal-semiconductor interfaces, the potential barrier of electrons is dictated primarily by the difference between the metal E_F and the CNT electron affinity. Accordingly, the gap of the semiconducting CNT, which is roughly inversely proportional to its diameter, is an important factor for determining the barrier for holes. Recently, a correlation has been shown between the diameter of the CNT and the on current for negative gate voltage of the device fabricated therein. Specifically, the on current increases with increasing CNT diameter.[11] Also, the work function of the metal electrodes has been shown to affect the device performance in a number of interesting ways. For instance, a metal electrode with a large work function, e.g., Pd, is shown to induce large on currents for holes,[12] while metal electrodes having small work functions, e.g., Al, enhance the on current of electrons.[13] When E_F lies near the midgap for intermediate values of the work function, the device is shown to exhibit an ambipolar behavior.[3,7,13]

Early theoretical work discussed the apparent validity of the Mott-Schottky picture in CNT transistors.[14] However, this simple picture cannot account for the general features of observed *I-V* characteristics: (i) why the on current does not scale exponentially with the work function in large band gap CNT's[11] and (ii) why the metal electrodes having similar work function induce different *I-V* behaviors. Specifically, Pd and Au have the same work function, but in Pd-contacted CNT's, the hole on current was in the microampere range,[12] whereas that attained in Au-contacted CNT's was in the nanoampere range.[9] In fact, a perfect transparency was reported in Pd contacted small gap CNT's[12] which was attributed to the formation of Ohmic contact for hole transport.[12] However, this also raises an interesting question, namely, why the same Ohmic contact has not been achieved with Au, having the same work function as Pd or with Pt,[15] which has a larger work function for that matter.

We present in this work a first-principles evaluation of the transport properties of large band-gap end-contacted CNT's. We considered two different contact models, one intentionally taken simple and one more realistic where we allow the chemical bonding at the surface to fully develop via the relaxation of contacting atomic positions. In an earlier work, it was shown that relaxation of the atomic positions of both the CNT and metal electrodes leads to distinct differences in the electronic structure of the contacting region of the CNT.[16] We have chosen for investigation Pd and Au electrodes since these metals are often utilized for device fabrication and have the same work function, but induce drastically different device performances. The experimental data are elucidated using the calculated transmission curves, density of states (DOS), and E_F location within the gap. In particular, the E_F location is shown to be determined by both the metal-induced DOS in the gap of the CNT, which accomodates most of the interface charge dipole, and by the intrinsic CNT end states, which pin E_F close to the midgap in the more simple contact models. For the more realistic contacts studied, the net differentation between metal-induced and end states disappears and the location of E_F turns out to be fairly similar for Au and Pd, as expected from the similar values of their respective work functions. Interestingly, however, the CNT contacted to Pd is highly transparent for hole injection, providing the maximum possible conductance of $4e^2/h$ at energies close to the valence band edge, while this is not the case for Au.

The transport calculations presented in this work are

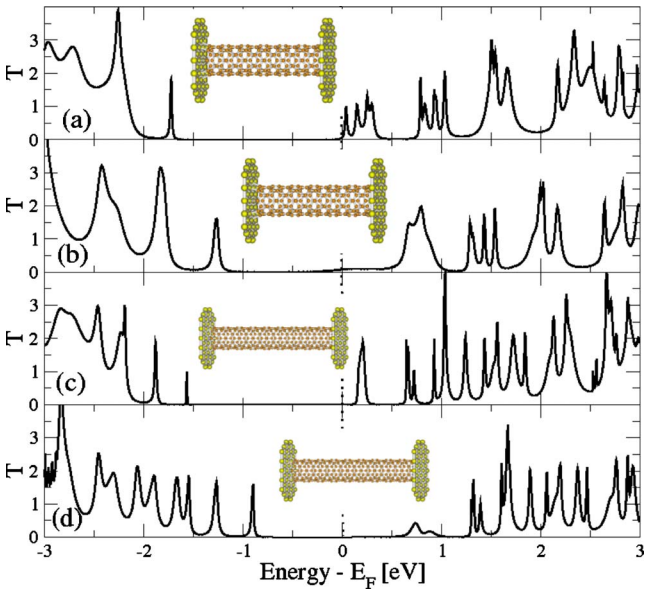

FIG. 1. (Color online) Transmission for an (8,0) CNT composed of six unit cells contacted to (a) Au and (b) Pd, as shown in the inset. Panels (c) and (d) show the same but for a nine unit-cell CNT.

based on the quantum transport package ALACANT.[17] The Kohn-Sham Green's function of the semiconducting CNT and a significant part of the electrodes (see insets in Figs. 1 and 3) is evaluated self-consistently with boundary conditions given by a parametrized description of the bulk electrodes implemented with the use of a Bethe lattice tight-binding model.[18,19] Other computational details are similar to those in Ref. 20.

Figure 1 shows the transmission spectra of a (8,0) six unit-cell (UC) and of a nine UC CNT with its open ends contacted to Au and Pd (111) layers, as shown in the insets. To single out the influence of the electronic structure of the metal atoms from that of the contact geometry, we have considered an ideal and simple contact model for both cases in which electrode and CNT planes are kept at a fixed distance of 2.2 Å, i.e., in an unoptimized electronic coupling configuration. The peaks are the result of resonant transmission through quasi-bound states associated with the discrete set of allowed values of the longitudinal k vector due to the finite length of the CNT. Although not shown herein, our calculations for infinite CNT's reveal two twofold degenerate valence bands and a much larger number of conduction bands in the energy range shown in this figure. This explains the dense transmission spectrum above the gap and the sparse spectrum below. Here, one can easily establish a one-to-one correspondence between peaks and discrete states belonging to the valence band. As the nanotube grows longer, the highest energy peak below the gap approaches the top of the valence band of the infinite CNT. The same applies to the lowest energy peak above the gap, but referred to the conduction band. For the nine UC CNT, the apparent gap in Fig. 1 is already close to the bulk gap (≈1.8 eV).

A closer look reveals a finite transmission in the gap for both metals,[21–23] which, as can be seen in Fig. 1, is marginal for the nine UC CNT. The physical origin of this transmission can be clarified with the aid of Fig. 2, where the DOS projected on successive carbon rings from the interface is plotted for the nine UC CNT. The DOS shows a broadened set of peaks in the gap which decays into the CNT bulk, the decaying length being longer for Au than for Pd. These states are commonly referred to as metal induced gap states,[14] but we would rather refer to them as surface or end states since they exist regardless of the metal. In fact, calculations of finite CNT's (terminated by H atoms to simulate the bonding to the surface) reveal four slowly decaying (≈2 nm) surface states in the gap. The finite and nearly constant DOS at the first interface C ring is apparently due to the chemical bonding between C and metal atoms. A fully developed energy gap is already visible from the third C ring on and no band bending can be seen,[22] at least at these length scales.[14]

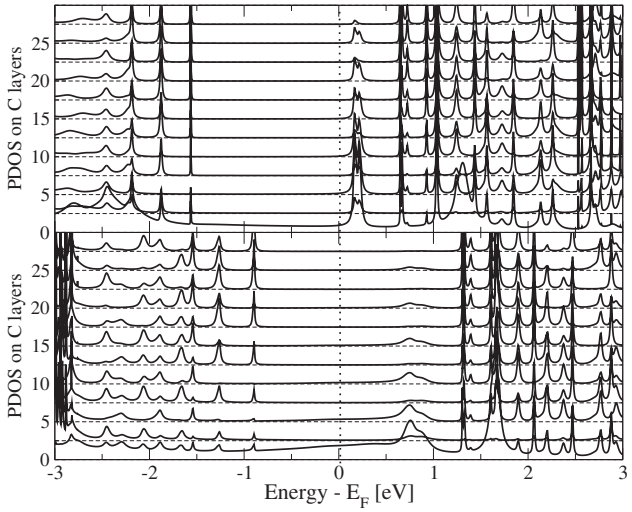

FIG. 2. Density of states projected on succesive carbon rings starting from the interface for the (c) (upper panel) and (d) (lower panel) cases shown in Fig. 1. Similar features are obtained for (a) and (b).

We note that E_F always lies below the lower edge of the surface state band for both Pd and Au contacts. The location of E_F is primarily determined by the contact-induced DOS at the first C layer which accomodates most of the charge transferred (from the metal to the CNT in the cases studied). Within the inherent uncertainty to Mulliken population analysis, the charge transferred is essentially the same for both metals (≈4 electrons for Au and ≈3.8 for Pd), but the metal-induced DOS is smaller for Au than for Pd (see Fig. 2). As a consequence, the Fermi level moves up within the gap in the former case until it gets pinned by surface states, as shown in Figs. 1(a) and 1(c). Since the surface state band arises from fairly extended surface states, if E_F lies above the band, allowing thereby electrons occupying these gap states, the excess charge would render the interface chemical bonding unstable.[21] This clearly shows the consistency of our computational results of charge redistribution accompanying the metal contact. The noticeable differences in the SB's associated with Au and Pd, however, do not seem to hold for more realistic contact models (see below).

Not only the DOS induced in the gap by the two metals is

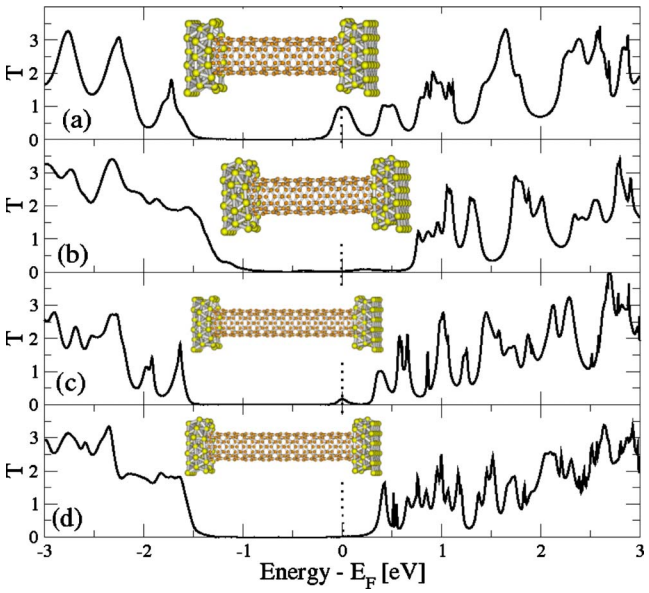

FIG. 3. (Color online) Transmission for six [(a) and (b)] and nine [(c) and (d)] unit-cell (8,0) CNTs contacted to Au [(a) and (c)] and Pd [(b) and (d)] electrodes as shown in the inset. The nanotube ends are embedded in the metal one atom layer deep.

different. They also induce a distinctly different transmission. The CNT-Pd system exhibits broader peaks below the gap which indicates a stronger hybridization strength of Pd atoms at these energies and it points to the importance of electronic coupling operative at the surface. We thus consider now a more realistic embedded contact geometry in which the end layers of the CNT are dipped into Pd and Au electrodes (see insets in Fig. 3). (Experimental evidence that electrical contact only occurs at the edge of the metal electrode[15] in part supports this contact model, although in real devices the CNT is deeply buried into the electrode.[24]) In this case, the surface atomic contact has been optimized, i.e., the atomic positions are allowed to relax to render the minimum energy and an optimized coupling. Note the drastic improvement of the transmission especially in the Pd-contacted CNT's compared to that shown in Fig. 1. The resonant transmission peaks appearing close to the valence band edge in Fig. 1 are here practically fused into a flat transmission spectrum reaching the maximum possible value of 2 (equivalent to a conductance of $4e^2/h$) [Figs. 3(b) and 3(d)]. For the case of Au, the improvement is there but the effect is not as conspicuous as in Pd. These improved transport properties can be attributed to (i) increased contact area due to the embedded geometry, hence more extensive hybridization, and (ii) the optimized atomic configurations enabling maximum chemical bonding at the surface. These effects will be further discussed in correlation with Fig. 4. The transmission in the conduction band is, on the other hand, not significantly affected by the relaxed atomic configurations. The location of E_F in the gap is now fairly similar for both Au and Pd electrodes and lies closer to the conduction edge due to a larger charge transfer.

Figures 4(a) and 4(b) show the cross-sectional profiles of the optimized atomic configurations and the associated

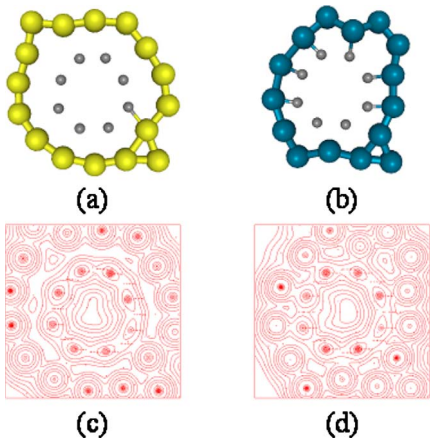

FIG. 4. (Color online) Atomic cross section of the metal-CNT interface for (a) Au and (b) Pd electrodes. Contour density plot at the interface for (c) Au and (d) Pd.

charge distribution [(c) and (d) panels] in the embedded layers for Au and Pd. Note the drastic differences in hybridization, specifically a strong chemical bonding for the case of Pd and a relatively weak bonding for Au. The surface atoms of gold exhibit a reduced *d* delocalization and *sd* hybridization.[25] On the other hand, the enhanced *sd* hybridization and the concomitant delocalization of the *d* electrons ensure that the repulsion between the Pd and C atoms of the CNT is much smaller than that between Au and C atoms.[26,27] Consequently, the Pd atoms are more strongly bound to the surface of the CNT.[28,29] This results in an enhanced charge redistribution at the Pd-C interface than at the Au-C interface [see Figs. 4(b) and 4(d)]. The improved charge exchange at the Pd-C interface also leads to an enhanced redistribution of the electron density of the contacting layer of the CNT.[16] An additional effect of *sd* hybridization in Pd is that its Fermi surface is almost entirely composed of *d*-like states,[26] while that of Au is composed of *s*-like states, with *d* DOS lying below E_F by about 2 eV.[30] The surface bonding is thus expected to give rise to substantial changes in the electronic contact properties of a CNT due to the extended nature of hybridized states as confirmed evidently in Fig. 3.

We have examined metal-contacted small-diameter CNT's in which case E_F lies mainly in the gap at the interface, as confirmed by experiments.[11] The precise location of E_F in the gap depends on the CNT surface DOS, which presents strong pinning properties, and on the highly localized metal-induced DOS, with much weaker pinning attributes. Both, in turn, strongly depend on the details of atomic structure of the contact, making it difficult to extract universal conclusions. For the, apparently, more realistic cases studied, we have not found significant differences between the respective SB's of Pd and Au. Keeping in mind that the location of E_F in the gap is, in general, a key factor dictating the contact resistance, barrier potential, and the overall device performance, the observed superior performance of the Pd-contacted *p*-channel CNT field effect transistor could be attributed to the stronger electronic coupling at the surface and not to a smaller SB compared to other metals of similar work function such as Au. Moreover, as experimentally reported,[12] a

perfect transparency for hole injection in Pd-contacted CNT's is found for a realistic contact model.

To conclude, since Schottky contacts are an integral part of the device, strongly influencing the transistor action, their role needs to be further investigated, in particular, in correlation with the chemical nature of surface electronic coupling and the sticking properties of metal atoms to the CNT. Additionally, the surface band bending should be analyzed together with the effect of both a transverse and a longitudinal electric field as induced by the gate and drain voltages. The obtained perfect transparency for hole injection in the case of Pd, being of chemical nature, is not expected to drastically change under the influence of these fields. Finally, the device performance should be further investigated as a function of the diameter and length of the CNT. All these factors are crucial for understanding the operational principle of the device and formulating a compact *I*-*V* model.

J.J.P. acknowledges discussions with F. Leonard and J. Fernández-Rossier. This work has been funded by the Spanish MEC under Grant Nos. FIS2004-02356, MAT2007-65487, and CONSOLIDER CSD2007-00010. P.T. and D.M.K. acknowledge the computational resources provided under the KISTI strategic support program.

[1] S. J. Tans, M. H. Devoret, R. J. A. Groeneveld, and C. Dekker, Nature (London) **394**, 761 (1998).
[2] R. Martel, T. Schmidt, H. R. Shea, T. Hertel, and P. Avouris, Appl. Phys. Lett. **73**, 2447 (1998).
[3] R. Martel, V. Derycke, C. Lavoie, J. Appenzeller, K. K. Chan, J. Tersoff, and P. Avouris, Phys. Rev. Lett. **87**, 256805 (2001).
[4] V. Derycke, R. Martel, J. Appenzeller, and P. Avouris, Nano Lett. **1**, 453 (2001).
[5] S. Heinze, J. Tersoff, R. Martel, V. Derycke, J. Appenzeller, and P. Avouris, Phys. Rev. Lett. **89**, 106801 (2002).
[6] J. Appenzeller, J. Knoch, V. Derycke, R. Martel, S. Wind, and P. Avouris, Phys. Rev. Lett. **89**, 126801 (2002).
[7] A. Javey, M. Shim, and H. Dai, Appl. Phys. Lett. **80**, 1064 (2002).
[8] S. J. Wind, J. Appenzeller, R. Martel, V. Derycke, and P. Avouris, Appl. Phys. Lett. **80**, 3817 (2002).
[9] V. Derycke, R. Martel, J. Appenzeller, and P. Avouris, Appl. Phys. Lett. **80**, 2773 (2002).
[10] X. Cui, M. Freitag, R. Martel, L. Brus, and P. Avouris, Nano Lett. **3**, 783 (2003).
[11] Z. Chen, J. Appenzeller, J. Knoch, Yu-Ming Lin, and P. Avouris, Nano Lett. **5**, 1497 (2005).
[12] A. Javey, J. Guo, Q. Wang, M. Lundstrom, and H. Dai, Nature (London) **424**, 654 (2003).
[13] M. H. Yang, K. B. K. Teo, W. I. Milne, and D. G. Hasko, Appl. Phys. Lett. **87**, 253116 (2005).
[14] F. Leonard and J. Tersoff, Phys. Rev. Lett. **84**, 4693 (2000).
[15] D. Mann, A. Javey, J. Kong, Q. Wang, and H. Dai, Nano Lett. **3**, 1541 (2003).
[16] D. M. K. P. Tarakeshwar, J. Phys. Chem. B **109**, 7601 (2005).
[17] J. J. Palacios, D. Jacob, A. J. Pérez-Jiménez, E. SanFabián, E. Louis, and J. A. Vergés, ALACANT, *ab initio* transport package, Release 1.1.5, Universidad de Alicante (http://www.guirisystems.com/alacant).
[18] J. J. Palacios, A. J. Pérez-Jiménez, E. Louis, and J. A. Vergés, Phys. Rev. B **64**, 115411 (2001).
[19] J. J. Palacios, A. J. Pérez-Jiménez, E. Louis, E. SanFabián, and J. A. Vergés, Phys. Rev. B **66**, 035322 (2002).
[20] J. J. Palacios, A. J. Pérez-Jiménez, E. Louis, E. SanFabián, and J. A. Vergés, Phys. Rev. Lett. **90**, 106801 (2003).
[21] P. Pomorski, C. Roland, and H. Guo, Phys. Rev. B **70**, 115408 (2004).
[22] Y. Xue and M. A. Ratner, Phys. Rev. B **70**, 205416 (2004).
[23] A. Rochefort, M. D. Ventra, and P. Avouris, Appl. Phys. Lett. **78**, 2521 (2001).
[24] W. Zhu and E. Kaxiras, Nano Lett. **6**, 1415 (2006).
[25] P. H. Citrin, G. K. Wertheim, and Y. Baer, Phys. Rev. Lett. **41**, 1425 (1978).
[26] F. M. Mueller, A. J. Freeman, J. O. Dimmock, and A. M. Furdyna, Phys. Rev. B **1**, 4617 (1970).
[27] S. G. Louie, Phys. Rev. Lett. **40**, 1525 (1978).
[28] E. Durgun, S. Dag, V. M. K. Bagci, O. Gülseren, T. Yildirim, and S. Ciraci, Phys. Rev. B **67**, 201401(R) (2003).
[29] A. Maiti and A. Ricca, Chem. Phys. Lett. **395**, 7 (2004).
[30] D. A. Shirley, Phys. Rev. B **5**, 4709 (1972).